ACS OMEGA

Open Access

http://pubs.acs.org/journal/acsodf

Article

Combined Experimental and Theoretical Study of the Synthesis of 5,7-Dihydroxy-4-methylcoumarin via a Pechmann Condensation in the Presence of UiO-66-SO_3H Catalysts

Pattraporn Srirattanasakunsuk, Bundet Boekfa,* Piti Treesukol, Nongpanga Jarussophon, Thana Maihom, Kanokwan Kongpatpanich, and Jumras Limtrakul

Cite This: *ACS Omega* 2023, 8, 46904−46913

Read Online

ACCESS | Metrics & More | Article Recommendations | Supporting Information

ABSTRACT: An efficient synthesis of 5,7-dihydroxy-4-methylcoumarin from phloroglucinol with ethyl acetoacetate in the UiO-66-SO_3H metal−organic framework is reported. The potential of UiO-66-SO_3H as a solid catalyst was determined through optimized-condition experiments and quantum molecular calculations. The optimal conditions for the synthesis of 5,7-dihydroxy-4-methylcoumarin with UiO-66-SO_3H were as follows: phloroglucinol/ethyl acetoacetate molar ratio = 1:1.6, reaction time = 4 h, and temperature = 140 °C, for which the reaction yield reached 66.0%. The reusability of UiO-66-SO_3H catalysts for Pechmann condensation was examined. The activation energy of the reaction occurring on a sulfonic group of the UiO-66-SO_3H catalyst was 12.6 kcal/mol, which was significantly lower than 22.6 kcal/mol of the same reaction on the UiO-66 catalyst. To comprehend the reaction mechanism, density functional theory with the ONIOM approach was applied for the synthesis of coumarin on the UiO-66-SO_3H and UiO-66 clusters. A possible reaction mechanism was proposed involving three steps: a trans-esterification step, an intramolecular hydroxyalkylation step, and a dehydration step. The rate-determining step was suggested to be the first step which acquired an activation energy of 15.7 and 29.5 kcal/mol, respectively. Information from this study can be used as guidelines to develop more efficient catalytic metal−organic frameworks for various organic syntheses.

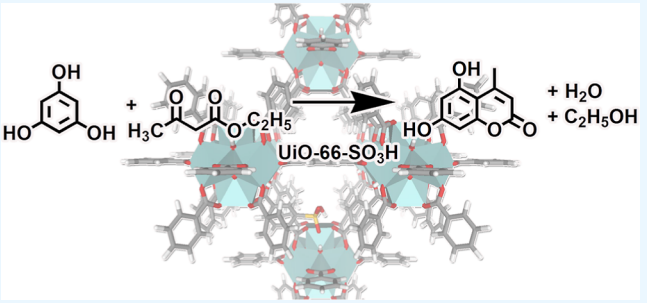

1. INTRODUCTION

Metal−organic frameworks (MOFs) are materials that have received significant attention for their potential applications as adsorbents and catalysts.[1−4] Generally, they have been widely used for applications such as gas storage and catalysts.[4] MOFs are constructed with large pore sizes and specific surface properties, that can be extensively modified by altering the metal center and unsaturated organic linker. The functionalization of MOFs with various reactive species can enhance their catalytic efficiency across various chemical reactions. MOFs with Brønsted acidity at the organic linker exhibit higher catalytic activity without compromising their catalytic stability and other physical properties.[4] Numerous reactions catalyzed by sulfonic groups as the Brønsted acid site over the organic linker of MOF have been investigated. Among these, an isoreticular Zr-MOF, namely UiO-66 synthesized with different linker ligands has been used as catalysts for various reactions with high thermal and chemical stabilities.[5,6] UiO-66 and defective UiO-66 have been applied for the glucose conversion.[7] Both UiO-66 and UiO-66-SO_3H have been successfully used to catalyze organic reactions such as isomerization, green synthesis, and condensation.[6,8−10] Recently, UiO-66 has been employed for hydroxylation and used for luminescent properties.[11,12]

Coumarin and its derivatives are important organic compounds used in various applications including food additives, cosmetics, agrochemicals, laser dyes, and medicines, especially for tumor and anti-HIV therapies.[13,14] Coumarin can be synthesized through conventional routes such as the Friedländer reaction,[15] Knoevenagel condensation,[16] and Pechmann condensation.[13,17] Among these, the Pechmann condensation reaction stands out of its simplicity and ability to yield various substituted coumarins with high efficiency. The reaction proceeds through a three-step mechanism: (1) transesterification of the phenol with ethyl acetoacetate, (2) intramolecular hydroxyalkylation, and (3) dehydration. In the past, conventional homogeneous catalysts such as sulfuric acid[13] and trifluoroacetic acid[18] were used in the Pechmann condensation, but they caused issues related to corrosion and

Received: September 2, 2023
Revised: October 9, 2023
Accepted: November 15, 2023
Published: November 30, 2023

reusability. Consequently, these acidic homogeneous catalysts have been significantly replaced by reusable heterogeneous catalysts such as zeolites[19−22] and MOFs.[23]

Various heterogeneous catalysts, including E4a,[24] 13X, H-FAU, H-Beta,[20,22] nanosponge zeolite,[25] and MOFs,[23] have been employed in coumarins' synthesis. Zeolites have been utilized for thio coumarin synthesis.[26] The synthesis of 7-hydroxy-4-methyl coumarin from resorcinol and ethyl acetoacetate using H-Beta was previously reported.[22] Various zeolite frameworks have the capability to stabilize the adsorption complexes and also to reduce activation barriers in the Pechmann condensation reaction. Zeolites have gained significant attention due to their catalytic performance and reusable capacity in various organic reactions, such as the dehydration reaction, hydrocarbon cracking, and esterification.[19,21] However, investigation of the Pechmann condensation reaction within the UiO-66 MOF remains limited.

Understanding the molecular adsorptions and reaction mechanisms within the large pores of zeolites or MOFs is necessary for improving their catalytic performance.[27] The investigation of adsorption and reaction mechanisms within these catalysts was conducted by using density functional theory (DFT). DFT with M06 functional, in which the confinement effect was taken into account, has proven effective in studying the adsorption and reactions within UiO-66 catalysts and other heterogeneous catalysts.[28−32] This DFT functional was also applied to examine the reaction of 7-hydroxy-4-methylcoumarin synthesis using Beta zeolite.[22] Structures and reactions within heterogeneous catalysts were studied with the ONIOM approach.[28,29] This method involved treating the active site and its related complexes with a high-accuracy level of calculation while employing a lower-accuracy calculation to depict the extended framework and represent the confinement effects of the environment.

In this study, the Pechmann condensation reaction catalyzed by the UiO-66-SO_3H MOF to produce 5,7-dihydroxy-4-methylcoumarin from phloroglucinol and ethyl acetoacetate was studied by experimental and theoretical approaches as shown in Scheme 1. Our study aimed to explore the Pechmann condensation reaction using UiO-66-SO_3H under optimal conditions and investigate the reaction mechanism. The impact of the Brønsted acid effect at the sulfonic group of UiO-66-SO_3H was evaluated through a comparison with the acid site at the metal site of UiO-66. Reactions were executed at varying temperatures, reaction times, and molar ratios of the substrate under solvent-free conditions. The products were characterized using thin layer chromatography (TLC), infrared spectroscopy (IR), and nuclear magnetic resonance (NMR) spectroscopy. Spectroscopic data from experimental observation and quantum calculation were compared. The adsorption and reaction mechanism of phloroglucinol with ethyl acetoacetate over UiO-66-SO_3H have been theoretically determined by using the ONIOM approach. The activation energy and reaction mechanism determined by experimental and theoretical studies of UiO-66-SO_3H and UiO-66 were discussed in detail.

Scheme 1. Reaction of 5,7-Dihydroxy-4-methylcoumarin Using Phloroglucinol and Ethyl Acetoacetate with UiO-66-SO_3H

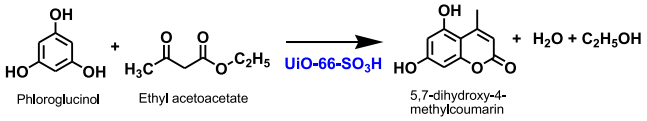

2. METHODOLOGY

2.1. Experimental Section. *2.1.1. Materials.* All Chemicals were obtained commercially and used without modification. UiO-66 was synthesized by dissolving $ZrCl_4$ (0.795 g, 3.4 mmol), 1,4-benzene dicarboxylic acid (BDC, 0.565 g, 3.4 mmol) in *N*,*N*-dimethylformamide (DMF, 135 mL), and glacial acetic acid (15 mL).[5,6,33,34] The mixture was then sonicated for 2 min and heated to 120 °C for 48 h. After cooling down to room temperature, the mixture was centrifuged and washed with DMF, acetone, and dried in a vacuum oven at 80 °C for 24 h. Similarly, UiO-66-SO_3H was synthesized by mixing $ZrCl_4$ (0.795 g, 3.4 mmol), BDC (0.462 g, 2.8 mmol), and monosodium 2-sulfoterephthalate (BDC.SO_3Na, 0.164 g, 0.6 mmol) in DMF (135 mL) and glacial acetic acid (15 mL). The remaining steps were followed as mentioned above, the same as those for UiO-66.

2.1.2. Instrumental Measurements. The structures and functional groups of the synthesized UiO-66-SO_3H and UiO-66 MOFs were characterized using X-ray diffraction (Bruker, D8 ADVANCE, Cu$K\alpha$ radiation), ^{1}H NMR spectroscopy (Bruker, D8 ADVANCE III HD, 600 MHz), and IR spectroscopy (PerkinElmer, Frontier FT-IR, Universal ATR). Nitrogen (N_2) sorption isotherms were measured using a MicrotracBEL BELSORP-mini X at −196 °C. The Brunauer−Emmett−Teller (BET) method was used to calculate the surface area, and the nonlocal DFT (NLDFT) models were used to evaluate the pore size distribution. The X-ray diffraction, IR spectrum, adsorption isotherms, and ^{1}H NMR of UiO-66 and UiO-66-SO_3H were measured, and the results are detailed in Figures S1−S8 in Supporting Information.

2.1.3. Catalytic Tests. To determine the catalytic activity of UiO-66 and UiO-66-SO_3H MOFs in the Pechmann condensation, reactions were conducted in a round-bottom flask by using an oil bath under controlled conditions. Specifically, a mixture of phloroglucinol (1.26 g, 10 mmol), ethyl acetoacetate (2.0 mL, 16 mmol), and 0.1 g of activated catalysts was stirred and refluxed at various temperatures (120−180 °C) and reaction times (1−8 h). Following the reaction, the reaction mixture was quenched by adding 10 mL of cold deionized water and then evaporated to dryness. After that, the coumarin product was dissolved in methanol, and the solid catalyst was filtered out. The coumarin product was purified by recrystallization with methanol. The purified product was characterized using TLC, melting point analysis, ^{1}H NMR spectroscopy, and IR spectroscopy. The percentage yield of the coumarin product was determined using the following equation

$$\text{percentage yield (\%)} = \left(\frac{\text{actual weight of product}}{\text{theoretical weight of product}}\right)\times 100 \quad (1)$$

The optimized conditions for the synthesis of coumarin using the UiO-66 and UiO-66-SO_3H catalysts were determined by testing the reaction at different temperatures and reaction times to identify the most optimum conditions yielding the highest percentage yield. The reaction rates were determined at different temperatures ranging from 120 to 140 °C for a duration of 4 h. To understand the catalytic behavior of the MOFs, kinetic rate constants and activation energies for the synthesis of coumarin

https://doi.org/10.1021/acsomega.3c06624
ACS Omega 2023, 8, 46904−46913

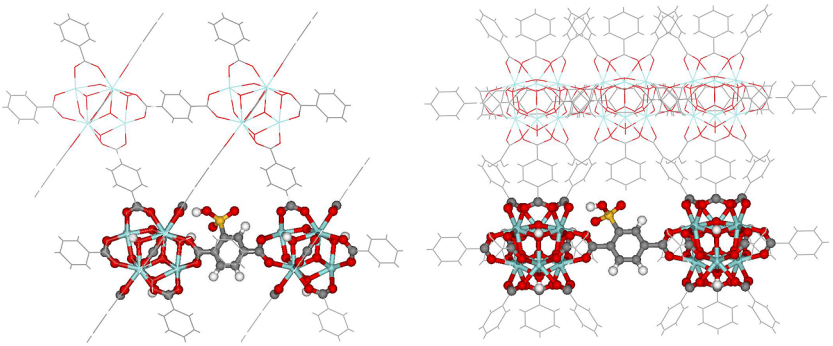

Figure 1. Optimized structures of UiO-66-SO_3H with the ONIOM(M06-L:PM6) approach.

on both UiO-66 and UiO-66-SO_3H catalysts were determined. The kinetic rate constants were experimentally measured at various temperatures while the activation energy (E_a) was calculated by using the Arrhenius equation as in eq 2

$$k = Ae^{-E_a/RT} \quad (2)$$

where k is the rate constant, A is the pre-exponential factor, E_a is the activation energy, R is the gas constant, and T is the temperature in kelvin. This information can be used to further understand the catalytic behavior of the MOFs and to identify the key factors that affect the efficiency of the catalysts. Additionally, it allows us to compare the activity of the two types of MOF catalysts.

To investigate the reusability of the UiO-66 and UiO-66-SO_3H catalysts, the synthesis of 5,7-dihydroxy-4-methylcoumarin from a 1:1.6 phloroglucinol/ethyl acetoacetate molar ratio was carried out at 140 °C for 4 h. After each reaction, the catalyst was separated and washed several times with hot ethanol and dried in an oven at 100 °C for 24 h. The catalytic activity of the reused UiO-66 catalysts was then compared with that of a conventional FAU zeolite (CBV720, Si/Al = 30) at the optimized conditions. Comparing the activity of the MOFs with conventional catalysts such as zeolites allows us to assess the performance of the MOFs in practical applications.

Physical and spectroscopic data of the 5,7-dihydroxy-4-methylcoumarin product from phloroglucinol and ethyl acetoacetate over UiO-66-SO_3H catalysts are as follows: light white solid; melting point: 282−284 °C; ^{1}H NMR (DMSO-d_6, 600 MHz): δ 2.49(d, J = 12 Hz, 3H,CH_3), 5.85(s, 1H, −H), 6.17 (s, 1H, Ar−H), 6.26 (s, 1H, Ar−H), 10.29(s, 1H, −OH), 10.51(s, 1H, −OH). IR(KBr): ν_{max} (cm^{-1}): 3406(OH), 3096 (═C−H), 2754 (−C−H), 1618 (lactone C═O), 1553−1464(C═C aromatic), and 1159 (C−O). The IR and NMR data of 5,7-dihydroxy-4-methylcoumarin product can be found in Figures S9−S12 in Supporting Information.

2.2. Theoretical. The Pechmann condensation reaction pathways for the synthesis of 5,7-dihydroxy-4-methylcoumarin using UiO-66-SO_3H and UiO-66 MOFs were proposed by using the ONIOM(M06-L:PM6) approach.[28] The UiO-66-SO_3H cluster was created from the unit cell of UiO-66.[35] The Zr_6O_8 clusters were connected to BDC or 5-sulfo-1,4-benzenedicarboxylate (BDC−SO_3H) to form a cubic nanoporous network with hydrogen-terminated BDC linkers. The large cluster of $(Zr_6O_4(OH)_4(CO_2)_{12})_6$ $(C_6H_3SO_3H)(C_6H_4)_{11}(-C_6H_5)_{48}$ covering the symmetrical six metal cluster node is shown in Figure 1. The active region, which covered two $Zr_6O_4(OH)_4(CO_2)_{12}$ clusters and one $C_6H_3SO_3H$ linker, was treated as the high-level region. The UiO-66 cluster was $(Zr_6O_4(OH)_4(CO_2)_{12})_6$ $(C_6H_4)_{12}(-C_6H_5)_{48}$. The high-level region was optimized using DFT with the M06-L functional,[36,37] while the extended cluster (the lower-level region) was kept fixed with the crystallographic structure and was treated with the semiempirical PM6 method.[38] During the optimization, the high-level region of UiO-66-SO_3H and the probe molecules were allowed to relax, while the rest were kept fixed with the crystallographic structure.

The M06-L DFT was used to study the reaction mechanism of the Pechmann condensation reaction of 5,7-dihydroxy-4-methylcoumarin synthesis with UiO-66-SO_3H MOF. To validate the calculation method, the M06-L functional was used to calculate the chemical properties of 5,7-dihydroxy-4-methylcoumarin and UiO-66-SO_3H and compare the calculated values with experimental values. The 6-31G(d,p) basis set was used for the C, H, O, and S atoms while the LANL2DZ basis set was employed for the Zr atoms. The single-point calculations were carried out at the high-level region and frequency calculations were performed at the same level of calculation. The thermal free energy to Gibbs free energies (G_{corr}) was calculated at 298.15 and 413.15 K and at a pressure of 1 atm. The electronic energies with free energies ($E_0 + G_{corr}$) were reported. All energies are reported in Table S1 in Supporting Information. The transition states with a single negative normal mode corresponding to the reaction pathway were determined by the Berny algorithm. All calculations were performed by using the Gaussian 09 program.[39]

3. RESULTS AND DISCUSSION

3.1. Synthesis and Characterization of Catalysts. The Pechmann condensation reaction of 5,7-dihydroxy-4-methylcoumarin was carried out from phloroglucinol and ethyl acetoacetate using UiO-66 and UiO-66-SO_3H catalysts, with the aim of understanding the influence of the Brønsted acidity from the sulfonic group and the confinement effect from the MOF catalysts in the reaction activity. UiO-66-SO_3H have been previously used in reactions such as the glucose isomerization.[6]

The results from X-ray diffraction of UiO-66 and UiO-66-SO_3H are shown in Figure S1 in Supporting Information. The sharp peaks from the XRD patterns of UiO-66 and UiO-66-SO_3H matched the UiO-66 structure.[12] The surface areas of UiO-66 and UiO-66-SO_3H were determined by analyzing the adsorption−desorption isotherms at 77 K as shown in Figure S3 in Supporting Information. The BET surface area, total pore volume, and micropore volume of UiO-66 were 1321 m^2 g^{-1}, 0.73 cm^3 g^{-1}, and 0.55 cm^3 g^{-1}, respectively, and those of UiO-66-SO_3H were 1102 m^2 g^{-1}, 0.72 cm^3 g^{-1}, and 0.34 cm^3 g^{-1}, respectively. The decrease in BET surface area suggested that

https://doi.org/10.1021/acsomega.3c06624
ACS Omega 2023, 8, 46904−46913

acidic groups were located inside the pore.[6,12] The ^{1}H NMR and IR spectroscopy, as shown in Figures S4, S5, and S7 in Supporting Information, indicated the differences between the linker's protons in UiO-66 and in UiO-66-SO_3H and confirmed the presence of the sulfonic group in UiO-66-SO_3H.

3.2. Catalytic Properties of UiO-66-SO_3H. The synthesis of 5,7-dihydroxy-4-methylcoumarin was conducted by using UiO-66-SO_3H under various conditions. The reaction was carried out in the liquid phase without solvent. By manipulating the chemical ratios, reaction times, and reaction temperatures, the optimal condition was determined as illustrated in entries 1−15 in Table 1. Ethyl acetoacetate dissolved phloroglucinol and diffused into the pores of the UiO-66-SO_3H catalyst. The most favorable condition with 0.1 g of the catalyst was identified as a 1:1.16 molar ratio of phloroglucinol to ethyl acetoacetate, resulting in a yield of 66.0%. Furthermore, the optimal reaction time for the synthesis of 5,7-dihydroxy-4-methylcoumarin with UiO-66-SO_3H was found to be 4 h at 140 °C.

Table 1. Screening for Optimal Conditions for the Synthesis of 5,7-Dihydroxy-4-methylcoumarin from Phloroglucinol and Ethyl Acetoacetate under Different Conditions with Several Catalysts

entry	mmol ratio[a]	catalyst[b]	temp (°C)	time (h)	yield (%)
1	1:1	UiO-66-SO_3H	140	4	30.5
2	1:1.2	UiO-66-SO_3H	140	4	40.5
3	1:1.6	UiO-66-SO_3H	140	4	66.0
4	1:2	UiO-66-SO_3H	140	4	43.6
5	1:3	UiO-66-SO_3H	140	4	36.5
6	1:1.6	UiO-66-SO_3H	120	4	29.2
7	1:1.6	UiO-66-SO_3H	125	4	38.3
8	1:1.6	UiO-66-SO_3H	130	4	46.2
9	1:1.6	UiO-66-SO_3H	135	4	51.5
10	1:1.6	UiO-66-SO_3H	160	4	68.6
11	1:1.6	UiO-66-SO_3H	180	4	71.8
12	1:1.6	UiO-66-SO_3H	140	1	30.6
13	1:1.6	UiO-66-SO_3H	140	2	41.2
14	1:1.6	UiO-66-SO_3H	140	6	62.4
15	1:1.6	UiO-66-SO_3H	140	8	63.4
16	1:1.6	UiO-66	120	4	13.7
17	1:1.6	UiO-66	125	4	16.6
18	1:1.6	UiO-66	130	4	23.6
19	1:1.6	UiO-66	135	4	36.9
20	1:1.6	UiO-66	140	4	49.3
21	1:1.6	H-FAU zeolite	140	4	58.1

[a]mmol ratio of phloroglucinol/ethyl acetoacetate. [b]Catalyst, 0.1 g.

The maximum percentage yield obtained using the UiO-66 catalyst was 49.3% (entries 16−20 in Table 1), significantly lower than 66.0% of the reaction with the UiO-66-SO_3H catalyst. Additionally, the catalytic activity of UiO-66-SO_3H was higher than that of the conventional FAU zeolite catalyst, which had a yield of 58% (entry 21 in Table 1). This highlights the effect of the Brønsted acidity from the sulfonic group and the potential of UiO-66-SO_3H as a highly active and efficient catalyst for the Pechmann condensation reaction.

The experimental activation energy was determined from reactions at temperatures 120−140 °C for 4 h to be 12.6 and 22.0 kcal/mol for UiO-66-SO_3H and UiO-66, respectively, as shown in Figure 2. The percent yield of coumarin product after reusing the MOF catalysts three times decreased slightly as shown in Figure 3. The decrease in reaction yield was attributed to the loss of some catalysts during the recovery process. After three reaction cycles, both the used UiO-66-SO_3H and UiO-66 catalysts exhibited similar structures and functional groups as depicted in Figures S2, S6, and S8 in Supporting Information. This indicated that both UiO-66-SO_3H and UiO-66 can be practically used to catalyze the Pechmann condensation of 5,7-dihydroxy-4-methylcoumarin, and the effect of the Brønsted acid from the sulfonic group can increase the reaction rate. The insertion of SO_3H groups into the framework of UiO-66 increased the acidity and reaction activity. This effect has been confirmed by results from various reactions, such as glucose-to-hydroxymethylfurfural transformation[6] where the yield increased from 2.7 to 14% when using UiO-66 and UiO-66-SO_3H, respectively. Similarly, in the *N*-formylation of aniline with formic acid,[40] the yield improved from less than 1−33% by utilizing UiO-66 and UiO-66-SO_3H, respectively. To comprehend the reaction mechanism responsible for enhancing the catalytic activity of UiO-66-SO_3H over UiO-66, we compared the results from the theoretical study with the experimental data in the following section.

3.3. DFT Calculation of the Reaction Mechanism. The Pechmann condensation of phloroglucinol with ethyl acetoacetate to 5,7-dihydroxy-4-methylcoumarin using UiO-66-SO_3H catalysts was studied using the ONIOM approach. The ONIOM(M06-L/6-31G(d,p):PM6) method was used to investigate the possible reaction mechanism. High activity of the Pechmann reaction for 5,7-dihydroxy-4-methylcoumarin inside UiO-66 catalysts was due to the bimolecular interaction of phloroglucinol and ethyl acetoacetate. The bimolecular process inside the MOF was previously suggested by the reaction on H-Beta zeolite[22] and CuBTC.[23] The proposed mechanism of the reaction with the UiO-66-SO_3H catalyst, shown in Scheme 2, suggested that the Brønsted acid of the sulfonic group in the UiO-66-SO_3H catalyst played an important role in the reaction by protonating to ethyl acetoacetate to interact with the phenol group of phloroglucinol to stabilize the formation of intermediate species followed by the dehydration to 5,7-dihydroxy-4-methylcoumarin.

To obtain reliable data on the performance of the M06-L functional, the calculated heat of reaction and NMR spectroscopy results were compared with those from the experiment and post Hartree−Fock calculation. The sum of electronic and thermal free energies determined from the M06-L DFT and MP2 calculation was compared. The reaction energy for phloroglucinol and ethyl acetoacetate to 5,7-dihydroxy-4-methylcoumarin, ethanol, and water was calculated to be 10.1 kcal/mol with M06-L/6-31G(d,p) and 13.1 kcal/mol calculated with MP2/6-311+G(2df,2p). The ^{1}H NMR shifts of 5,7-dihydroxy-4-methylcoumarin with δ = 4.91−6.21 ppm for H-3, H-6 and H-8, and 1.83−2.67 (3H, s, CH_3) determined from the M06-L method agreed well with experimental data of 5.85−6.26 ppm for H-3, H-6 and H-8, and 2.49−2.51 ppm. These chemical shifts also agreed well with the MP2 calculations of 5.81−7.33 ppm for H-3, H-6 and H-8, and 2.26−3.11 ppm. The experimental ^{1}H NMR peak at 10.29−10.51 ppm indicated the weak band interaction. The ^{1}H NMR chemical shift for UiO-66-SO_3H was calculated with the M06-L/6-31G(d,p) calculation. The ^{1}H NMR δ = 7.92−8.16 ppm for H of the BDC agreed well with experimental data of 7.32−8.40 ppm as shown in the Supporting Information. Overall, the calculated chemical shift and reaction energy from the M06-L functional agreed well with the experimental study and the MP2 calculations;

https://doi.org/10.1021/acsomega.3c06624
ACS Omega 2023, 8, 46904−46913

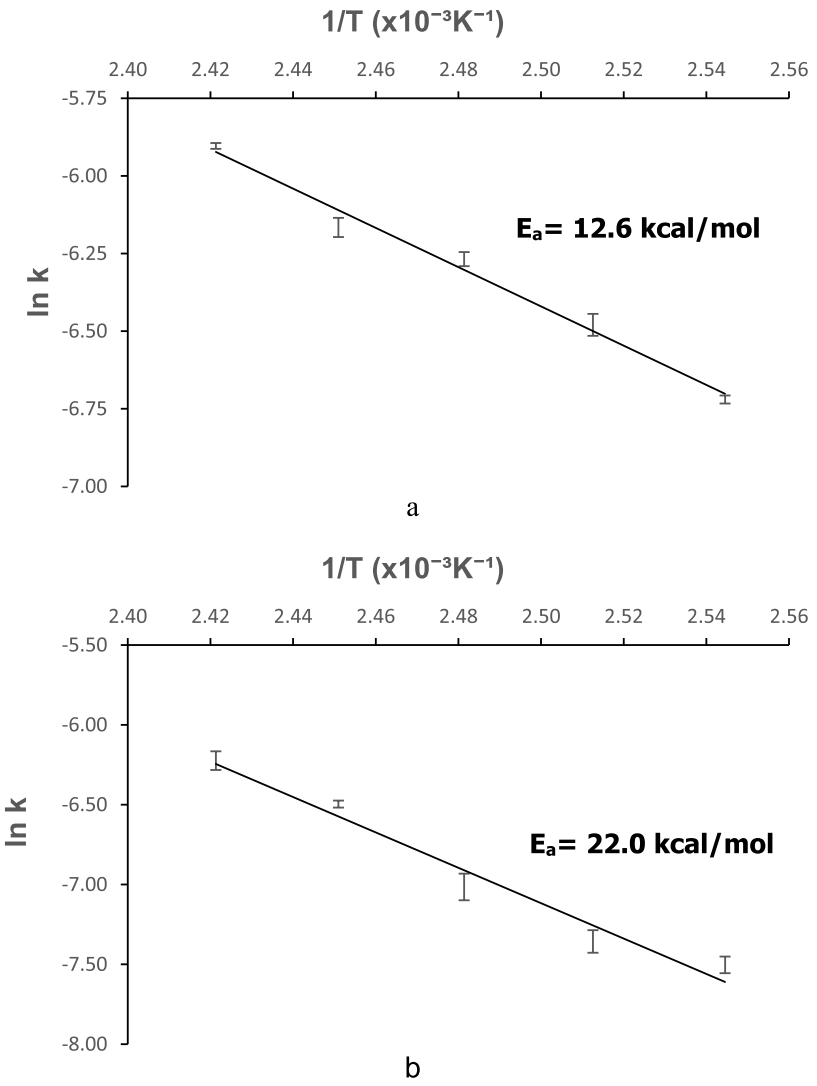

Figure 2. Arrhenius plots for the Pechmann condensation reaction on (a) UiO-66-SO_3H and (b) UiO-66 catalysts. The reaction was studied under the following condition: 10 mmol of phloroglucinol, 16 mmol of ethyl acetoacetate, 0.1 g of the catalyst, and a reaction time of 4 h.

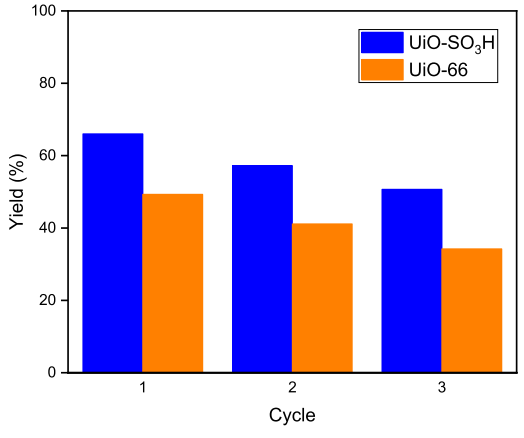

Figure 3. Reusability of UiO-66-SO_3H (blue) and UiO-66 (orange) catalysts in the context of the Pechmann condensation reaction. The reaction was studied under the following conditions: 10 mmol of phloroglucinol, 16 mmol of ethyl acetoacetate, 0.1 g of the catalyst, and a reaction time of 4 h.

therefore, it was further used for examining the reaction mechanism.

The UiO-66-SO_3H catalyst (Figure 1) was represented by an ONIOM(M06-L:PM6) cluster model. The high-level calculation region and relevant species were optimized to study the Pechmann condensation reaction of phloroglucinol and ethyl acetoacetate on the Brønsted acid sites of the UiO-66-SO_3H catalyst. The Pechmann condensation reaction was considered to proceed on the Brønsted acid of the sulfonic group of UiO-66-SO_3H. The reaction mechanism was proposed to be a three-step mechanism as shown in Scheme 2. The thermal Gibbs free energies of each step were reported at the same level of theory as shown in Table S1 in Supporting Information. Selected optimized structural parameters are shown in Table S2 in Supporting Information. First, the Brønsted acid of UiO-66-SO_3H catalyzed the transesterification step and produced the dihydroxyphenyl-3-oxobutanote intermediate and an ethanol. The optimized structure of coadsorption [AD1] of phloroglucinol and ethyl acetoacetate is shown in Figure 4. The relative energy (or adsorption energy) for the coadsorption step was −23.0 kcal/mol. The reaction proceeded via the C2−O bond-breaking and the O1−C2 bond-forming. At the transition state [TS1], the intermolecular distances of C2···O and O1···C2 were 2.21 and 1.75 Å, respectively. Single imaginary frequency from normal-mode analysis of this transition state was at 222.1i cm^{-1}

https://doi.org/10.1021/acsomega.3c06624
ACS Omega 2023, 8, 46904−46913

Scheme 2. Pechmann Condensation Reaction Mechanism of Phloroglucinol with Ethyl Acetoacetate to 5,7-Dihydroxy-4-methylcoumarin Using UiO-66-SO_3H Catalysts

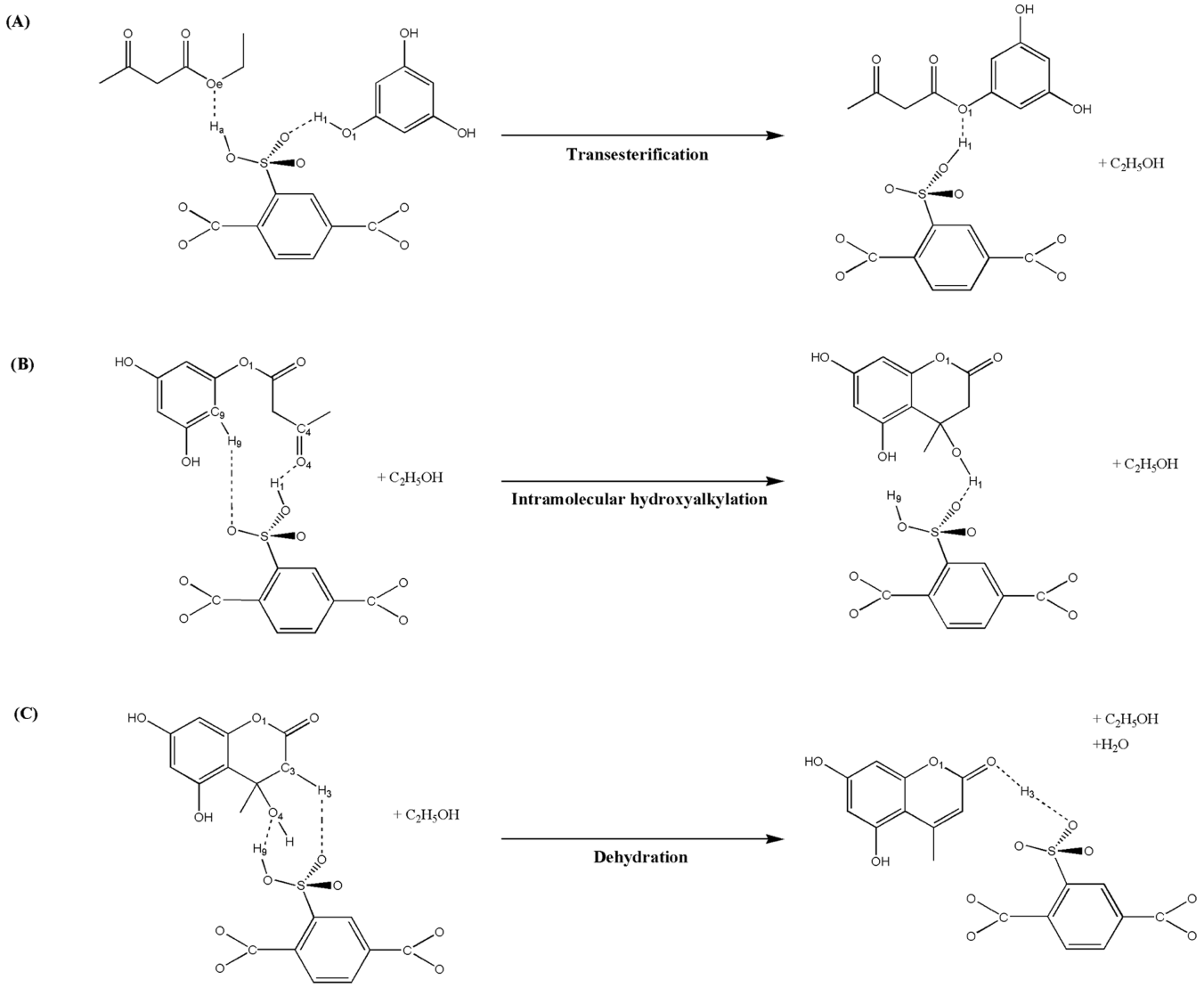

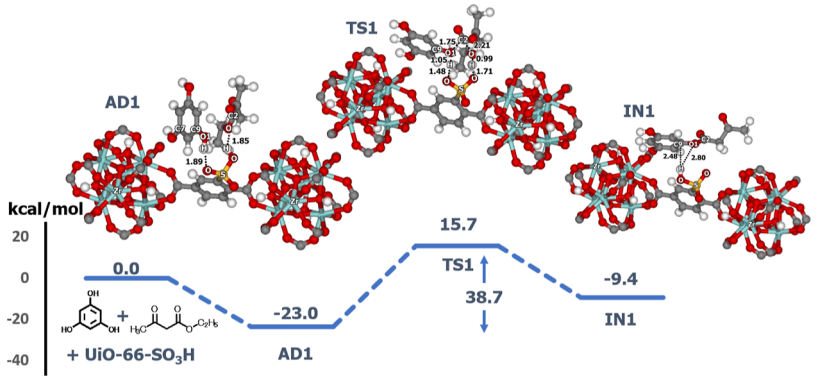

Figure 4. Reaction pathway for the transesterification step of the Pechmann condensation involving 5,7-dihydroxy-4-methylcoumarin from phloroglucinol and ethyl acetoacetate over UiO-66-SO_3H. The optimized structures of AD1, TS1, and IN1 were calculated using the ONIOM(M06-L:PM6) approach. Distances are expressed in Å, and energies are measured in kcal/mol.

and was related to the reaction pathway. This step was the rate-determining step, with a total activation energy of 38.7 kcal/mol. The apparent activation energy was determined to be 15.7 kcal/mol, which agreed well with the experimental value of 12.6 kcal/mol. The (3,5-dihydroxyphenyl)-3-oxobutanoate intermediate [IN1] was the product of this step with a relative energy of −9.4 kcal/mol. The transesterification step was previously reported to be the rate-determining step for the synthesis of 7-hydroxy-4-

https://doi.org/10.1021/acsomega.3c06624
ACS Omega 2023, 8, 46904−46913

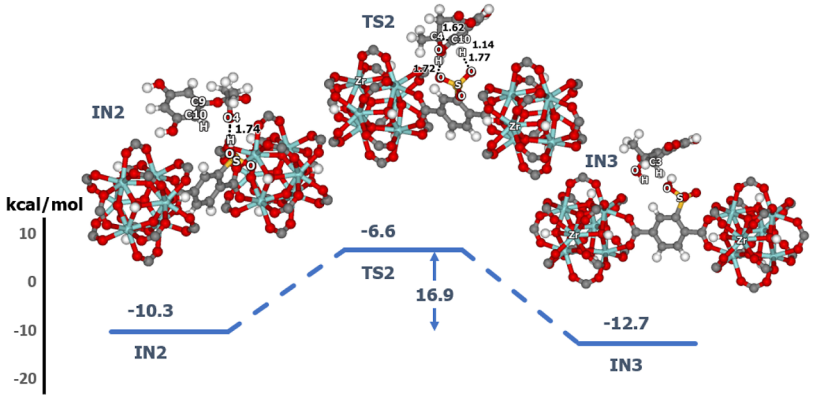

Figure 5. Reaction pathway for the intramolecular hydroxyalkylation step of the Pechmann condensation involving 5,7-dihydroxy-4-methylcoumarin from phloroglucinol and ethyl acetoacetate over UiO-66-SO_3H. The optimized structures of IN2, TS2, and IN3 were calculated using the ONIOM(M06-L:PM6) approach. Distances are expressed in Å and energies are measured in kcal/mol.

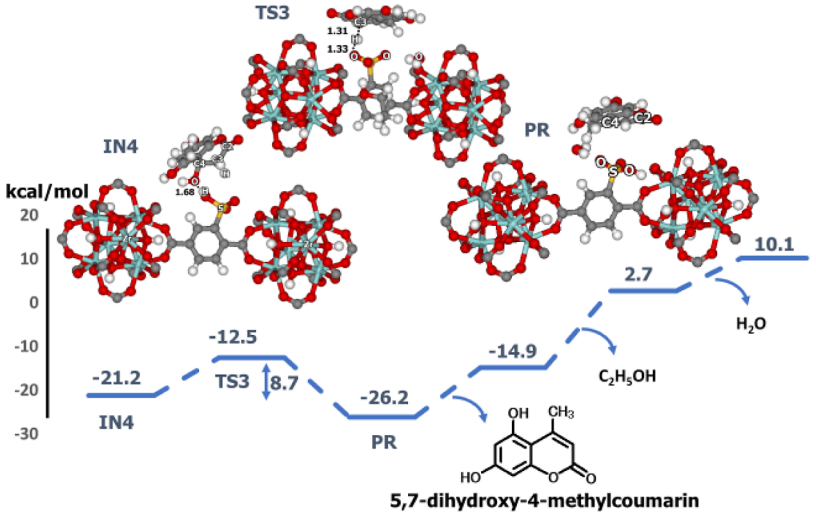

Figure 6. Reaction pathway for the dehydration step of the Pechmann condensation involving 5,7-dihydroxy-4-methylcoumarin from phloroglucinol and ethyl acetoacetate over UiO-66-SO_3H. The optimized structures of IN4, TS3, and PR were calculated by using the ONIOM(M06-L:PM6) approach. Distances are expressed in Å and energies are measured in kcal/mol.

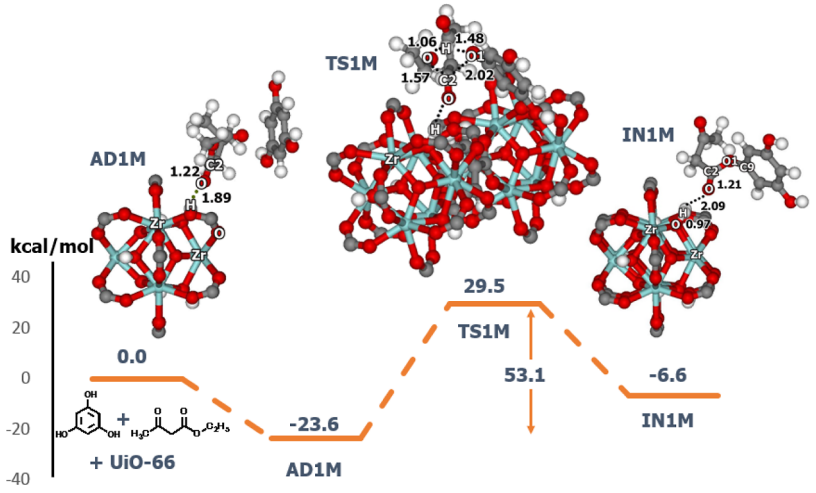

Figure 7. Reaction pathway for the transesterification step of the Pechmann condensation of 5,7-dihydroxy-4-methylcoumarin from phloroglucinol and ethyl acetoacetate over UiO-66. The optimized structures of AD1M, TS1M, and IN1M were calculated using the ONIOM(M06-L:PM6) approach. Distances are expressed in Å and energies are measured in kcal/mol.

methylcoumarin from resorcinol and ethyl acetoacetate with H_2SO_4 catalysts[13] and H-Beta zeolite[22] as well. Furthermore, the Gibbs free energies corresponding to two different temperatures, which align with our experimental conditions, are

https://doi.org/10.1021/acsomega.3c06624
ACS Omega 2023, 8, 46904−46913

presented in Table S1 in Supporting Information. The first step, identified as the rate-determining step, exhibits a barrier of 38.8 and 39.9 kcal/mol at 298.15 and 413.15 K, respectively.

Next, the intramolecular hydroxyalkylation from the carbonyl by electrophilic attack on the benzene ring was followed by rearomatization to from the coumarin skeleton. The reaction started from the (3,5-dihydroxyphenyl)-3-oxobutanoate intermediate (IN2) to produce the 3,4-dihydro-4,5,7-trihydroxy-4-methylchromen-2-one intermediate (IN3) as shown in the Figure 5. The IN2 complex was similar to the IN1 complex from the first step, but their alignment corresponded to the reaction pathway. The relative energy was about −10.3 kcal/mol. The C−C bond formation was found in this step with an activation energy of 16.9 kcal/mol. The product IN3 was released with a relative energy of −12.7 kcal/mol. The configuration of the product can be rearranged for the last step (IN4), the dehydration reaction, as shown in the Figure 6. The relative energy of this intermediate was −21.2 kcal/mol. The hydrogen bond interaction between the intermediate and the acid site increases the adsorption energy of this step. The interaction proceeded via the transition state (TS3) with a double proton transfer and C−O bond breaking. The total activation energy was 8.7 kcal/mol. The reaction produces 5,7-dihydroxy-4-methylcoumarin and water molecules with a relative energy of −26.2 kcal/mol. Single imaginary frequencies from normal-mode analysis of TS2 and TS3 were 92.7i and 219.4i cm^{-1}, respectively. These corresponded to the reaction pathway.

The reaction over the acid at the metal site of the UiO-66 catalyst was studied with the ONIOM approach. All reaction energies were calculated with an ONIOM (M06-L:PM6). The transesterification step, as shown in Figure 7, was the rate-determining step of the reaction. Ethyl acetoacetate preferred to adsorb close to the metal cluster of UiO-66 due to the strong interaction between the carbonyl group of ethyl acetoacetate and hydrogen at the metal site of UiO-66. The transition state [TS1M] presented the cyclic movement of four center atoms, including the breaking of the C2−O and O1−H bonds while the forming of the C2−O1 and the O−H bonds. This step had a single imaginary vibrational frequency at 580.7i cm^{-1}, corresponding to the reaction pathway. The reaction proceeds via C2−O and C2−O1 bond distances of 1.57 and 2.02 Å, respectively. The activation barrier was 53.1 kcal/mol, which was significantly higher than 38.7 kcal/mol of the reaction over a sulfonic group. The (3,5-dihydroxyphenyl)-3-oxobutanoate intermediate [IN1M] was the product of this step, with a relative energy of −6.6 kcal/mol. The calculated apparent activation energy for the reaction over UiO-66 was 29.5 kcal/mol, which was higher than that for UiO-66-SO_3H, which was calculated to be 15.7 kcal/mol. These calculated energies were in good agreement with experimental measurements of 22.0 and 12.6 kcal/mol for UiO-66 and UiO-66-SO_3H, respectively. These results showed that the Brønsted acid of the sulfonic group increased the activity of UiO-66 catalysts for the synthesis of coumarin.

4. CONCLUSIONS

In this study, the synthesis of coumarin was examined by a combination of experimental and theoretical studies. The UiO-66-SO_3H MOF has been used as a catalyst for the synthesis of 5,7-dihydroxy-4-methylcoumarin from phloroglucinol with ethyl acetoacetate. The UiO-66-SO_3H MOF was synthesized from the solvothermal method. The ^{1}H NMR, XRD, BET measurements, and IR spectroscopies were used to characterize the UiO-66-SO_3H catalysts and 5,7-dihydroxy-4-methylcoumarin product. The reactions were carried out with various molar ratios of phloroglucinol and ethyl acetoacetate (1:1, 1:1.2, 1:1.6, 1:2, and 1:3). The 1:1.6 mol ratio provided the highest yield with the optimum reaction time of 4 h with steady rate at 140 °C. The activation energies for the synthesis of coumarin on both UiO-66-SO_3H and UiO-66 catalysts were determined to be 12.6 and 22.0 kcal/mol, respectively. The catalysts were reused for three times with high percent yield.

The ONIOM approach was used to investigate the structure, adsorption, and reaction mechanism. The calculated chemical shift and reaction energy were determined with DFT M06-L which agreed well with experimental measurables and the MP2 results. The reaction mechanism was proposed to proceed on the Brønsted acid site of the sulfonic group of UiO-66-SO_3H with the three-step mechanism: a transesterification step, an intramolecular hydroxyalkylation step, and a dehydration step. The activation energies of each step were calculated to be 38.7, 16.9, and 8.7 kcal/mol, respectively. The reaction over the Brønsted acid site at the metal cluster of UiO-66 was examined. The apparent activation energy of 15.7 and 29.5 kcal/mol from the reaction over UiO-66-SO_3H and UiO-66 agreed well with experimental results. The UiO-66-SO_3H catalysts were suggested to be suitable for the synthesis of coumarin because of its highest percent yield, lowest activation barrier, and reusability.

■ ASSOCIATED CONTENT

Supporting Information

The Supporting Information is available free of charge at https://pubs.acs.org/doi/10.1021/acsomega.3c06624.

XRD pattern, N_2 adsorption−desorption isotherm, IR spectra of catalysts, ^{1}H NMR spectra, IR spectra of coumarin, optimized structures, energies, and structural parameters (PDF)

■ AUTHOR INFORMATION

Corresponding Author

Bundet Boekfa − *Division of Chemistry, Department of Physical and Material Sciences, Faculty of Liberal Arts and Science, Kasetsart University, Nakhon, Pathom 73140, Thailand; Center for Advanced Studies in Nanotechnology for Chemical, Food and Agricultural Industries, Kasetsart University Institute for Advanced Studies, Kasetsart University, Bangkok 10900, Thailand;* orcid.org/0000-0002-9281-9405; Email: bundet.b@ku.ac.th

Authors

Pattraporn Srirattanasakunsuk − *Division of Chemistry, Department of Physical and Material Sciences, Faculty of Liberal Arts and Science, Kasetsart University, Nakhon, Pathom 73140, Thailand; Department of Materials Science and Engineering, School of Molecular Science and Engineering, Vidyasirimedhi Institute of Science and Technology, Rayong 21210, Thailand*

Piti Treesukol − *Division of Chemistry, Department of Physical and Material Sciences, Faculty of Liberal Arts and Science, Kasetsart University, Nakhon, Pathom 73140, Thailand*

Nongpanga Jarussophon − *Division of Chemistry, Department of Physical and Material Sciences, Faculty of Liberal Arts and Science, Kasetsart University, Nakhon, Pathom 73140, Thailand*

https://doi.org/10.1021/acsomega.3c06624
ACS Omega 2023, 8, 46904−46913

Thana Maihom − *Division of Chemistry, Department of Physical and Material Sciences, Faculty of Liberal Arts and Science, Kasetsart University, Nakhon, Pathom 73140, Thailand;* orcid.org/0000-0002-8180-1218

Kanokwan Kongpatpanich − *Department of Materials Science and Engineering, School of Molecular Science and Engineering, Vidyasirimedhi Institute of Science and Technology, Rayong 21210, Thailand;* orcid.org/0000-0002-4353-7057

Jumras Limtrakul − *Department of Materials Science and Engineering, School of Molecular Science and Engineering, Vidyasirimedhi Institute of Science and Technology, Rayong 21210, Thailand*

Complete contact information is available at: https://pubs.acs.org/10.1021/acsomega.3c06624

Author Contributions

P.S. conducted laboratory work. B.B. was responsible for manuscript preparation, performing calculations, and conceptualization. P.T. provided editing support and formal analysis. N. J. conducted experimental and formal analysis. T.M. contributed to the formal analysis. K.K conducted experimental and formal analysis. J.L. was involved in the formal analysis. All authors discussed the results and contributed to the final manuscript.

Notes

The authors declare no competing financial interest.

■ ACKNOWLEDGMENTS

The project was funded by the National Research Council of Thailand (NRCT) and Kasetsart University grant N42A650283 to Bundet Boekfa. Pattraporn Srirattanasakunsuk acknowledges a Graduate School Kasetsart University. The support from Kasetsart University Research and Development Institute (KURDI) and the Faculty of Liberal Arts and Science Kasetsart University Kamphaeng Saen Campus are also acknowledged. This research has received funding support from the NSRF via the Program Management Unit for Human Resources & Institutional Development, Research, and Innovation, Thailand (grant number B40G660034). The authors acknowledge National e-Science Infrastructure Consortium and LANTA for providing computing resources that have contributed to the research results reported within this paper.

■ ABBREVIATIONS

MOFs, metal−organic frameworks; TLC, thin layer chromatography; XRD, X-ray diffraction; IR, infrared; NMR, nuclear magnetic resonance; BET, Brunauer−Emmett−Teller; DFT, density functional theory; ONIOM, our own N-layered integrated molecular orbital and molecular mechanics; MP2, second-order Møller−Plesset theory; M06-L, Minnesota 2006 local functional; PM6, parameterization method 6

■ REFERENCES

(1) Eddaoudi, M.; Kim, J.; Rosi, N.; Vodak, D.; Wachter, J.; O'Keeffe, M.; Yaghi, O. M. Systematic design of pore size and functionality in isoreticular MOFs and their application in methane storage. *Science* **2002**, *295* (5554), 469−472.

(2) Furukawa, H.; Cordova, K. E.; O'Keeffe, M.; Yaghi, O. M. The chemistry and applications of metal-organic frameworks. *Science* **2013**, *341* (6149), 1230444.

(3) Zhou, H. C. J.; Kitagawa, S. Metal-Organic Frameworks (MOFs). *Chem. Soc. Rev.* **2014**, *43* (16), 5415−5418.

(4) Lee, J.; Farha, O. K.; Roberts, J.; Scheidt, K. A.; Nguyen, S. T.; Hupp, J. T. Metal-organic framework materials as catalysts. *Chem. Soc. Rev.* **2009**, *38* (5), 1450−1459.

(5) Kandiah, M.; Nilsen, M. H.; Usseglio, S.; Jakobsen, S.; Olsbye, U.; Tilset, M.; Larabi, C.; Quadrelli, E. A.; Bonino, F.; Lillerud, K. P. Synthesis and stability of tagged UiO-66 Zr-MOFs. *Chem. Mater.* **2010**, *22* (24), 6632−6640.

(6) Tangsermvit, V.; Pila, T.; Boekfa, B.; Somjit, V.; Klysubun, W.; Limtrakul, J.; Horike, S.; Kongpatpanich, K. Incorporation of Al^{3+} Sites on Brønsted Acid Metal-Organic Frameworks for Glucose-to-Hydroxylmethylfurfural Transformation. *Small* **2021**, *17* (22), 2006541.

(7) Rojas-Buzo, S.; Corma, A.; Boronat, M.; Moliner, M. Unraveling the reaction mechanism and active sites of metal-organic frameworks for glucose transformations in water: Experimental and theoretical studies. *ACS Sustain. Chem. Eng.* **2020**, *8* (43), 16143−16155.

(8) Thongnuam, W.; Pornsatitworakul, S.; Maihom, T.; Treesukol, P.; Jarussophon, N.; Maitarad, P.; Kongpatpanich, K.; Boekfa, B. An experimental and theoretical study on the aldol condensation on zirconium-based metal-organic framework. *Key Eng. Mater.* **2017**, *757*, 98−102.

(9) Chen, J.; Li, K.; Chen, L.; Liu, R.; Huang, X.; Ye, D. Conversion of fructose into 5-hydroxymethylfurfural catalyzed by recyclable sulfonic acid-functionalized metal-organic frameworks. *Green Chem.* **2014**, *16* (5), 2490−2499.

(10) Ghorbani-Vaghei, R.; Azarifar, D. A. D.; Daliran, S.; Oveisi, A. R. The UiO-66-SO_3H metal-organic framework as a green catalyst for the facile synthesis of dihydro-2-oxypyrrole derivatives. *RSC Adv.* **2016**, *6* (35), 29182−29189.

(11) Kaiyasuan, C.; Somjit, V.; Boekfa, B.; Packwood, D.; Chasing, P.; Sudyoadsuk, T.; Kongpatpanich, K.; Promarak, V. Intrinsic Hole Mobility in Luminescent Metal-Organic Frameworks and Its Application in Organic Light-Emitting Diodes. *Angew. Chem., Int. Ed.* **2022**, *61* (18), No. e202117608.

(12) Somjit, V.; Thinsoongnoen, P.; Pila, T.; Boekfa, B.; Wannapaiboon, S.; Kongpatpanich, K. Hydroxylation of UiO-66 Metal-Organic Frameworks for High Arsenic(III) Removal Efficiency. *Inorg. Chem.* **2022**, *61* (29), 11342−11348.

(13) Pornsatitworakul, S.; Boekfa, B.; Maihom, T.; Treesukol, P.; Namuangruk, S.; Jarussophon, S.; Jarussophon, N.; Limtrakul, J. The coumarin synthesis: a combined experimental and theoretical study. *Monatsh. Chem.* **2017**, *148* (7), 1245−1250.

(14) Sethna, S. M.; Shah, N. M. The chemistry of coumarins. *Chem. Rev.* **1945**, *36* (1), 1−62.

(15) Perez-Mayoral, E.; Čejka, J. $[Cu_3(BTC)_2]$: A Metal-Organic Framework Catalyst for the Friedlander Reaction. *ChemCatChem* **2011**, *3* (1), 157−159.

(16) Ranu, B. C.; Jana, R. Ionic liquid as catalyst and reaction medium - A simple, efficient and green procedure for Knoevenagel condensation of aliphatic and aromatic carbonyl compounds using a task-specific basic ionic liquid. *Eur. J. Org Chem.* **2006**, *2006* (16), 3767−3770.

(17) von Pechmann, H. Neue Bildungsweise der Cumarine. Synthese des Daphnetins. I. *Ber. Dtsch. Chem. Ges.* **1884**, *17* (1), 929−936.

(18) Woods, L. L.; Sapp, J. A New One-Step Synthesis of Substituted Coumarins. *J. Org. Chem.* **1962**, *27* (10), 3703−3705.

(19) Venuto, P. B. Organic catalysis over zeolites: A perspective on reaction paths within micropores. *Microporous Mater.* **1994**, *2* (5), 297−411.

(20) Gunnewegh, E. A.; Hoefnagel, A. J.; van Bekkum, H. Zeolite catalysed synthesis of coumarin derivatives. *J. Mol. Catal. A: Chem.* **1995**, *100* (1−3), 87−92.

(21) Smit, B.; Maesen, T. L. M. Towards a Molecular Understanding of Shape Selectivity. *Nature* **2008**, *451* (7179), 671−678.

(22) Klinyod, S.; Boekfa, B.; Pornsatitworakul, S.; Maihom, T.; Jarussophon, N.; Treesukol, P.; Wattanakit, C.; Limtrakul, J. Theoretical and Experimental Study on the 7-Hydroxy-4-Methylcoumarin Synthesis with H-Beta Zeolite. *ChemistrySelect* **2019**, *4* (36), 10660−10667.

(23) Opanasenko, M.; Shamzhy, M.; Čejka, J. Solid Acid Catalysts for Coumarin Synthesis by the Pechmann Reaction: MOFs versus Zeolites. *ChemCatChem* **2013**, *5* (4), 1024−1031.
(24) Hegedüs, A.; Hell, Z. Zeolite-catalyzed Pechmann synthesis of coumarins. *Catal. Lett.* **2006**, *112* (1−2), 105−108.
(25) Kim, J. C.; Ryoo, R.; Opanasenko, M. V.; Shamzhy, M. V.; Čejka, J. Mesoporous MFI Zeolite Nanosponge as a High-Performance Catalyst in the Pechmann Condensation Reaction. *ACS Catal.* **2015**, *5* (4), 2596−2604.
(26) Zaitceva, O.; Bénéteau, V.; Ryabukhin, D. S.; Louis, B.; Vasilyev, A. V.; Pale, P. Zeolite-promoted Synthesis of Coumarins and Thiocoumarins. *ChemCatChem* **2020**, *12* (1), 326−333.
(27) Derouane, E. G. Zeolites as solid solvents "Paper presented at the International Symposium 'Organic Chemistry and Catalysis' on the occasion of the 65th birthday of Prof. H. van Bekkum, Delft, Netherlands, 2−3 October 1997.". *J. Mol. Catal. A: Chem.* **1998**, *134* (1−3), 29−45.
(28) Dapprich, S.; Komáromi, I.; Byun, K. S.; Morokuma, K.; Frisch, M. J. A new ONIOM implementation in Gaussian98. Part I. The calculation of energies, gradients, vibrational frequencies and electric field derivatives. *J. Mol. Struct.* **1999**, *461−462*, 1−21.
(29) Maeboonruan, N.; Boekfa, B.; Maihom, T.; Treesukol, P.; Kongpatpanich, K.; Namuangruk, S.; Probst, M.; Limtrakul, J. Adsorption and dehydration of ethanol on B, Al, and Ga substituted H-ZSM-5 zeolite: an embedded ONIOM study. *J. Mol. Model.* **2021**, *27* (12), 354.
(30) Zhao, P.; Boekfa, B.; Shimizu, K. I.; Ogura, M.; Ehara, M. Selective catalytic reduction of NO with NH_3 over Cu-exchanged CHA, GME, and AFX zeolites: a density functional theory study. *Catal. Sci. Technol.* **2021**, *11* (5), 1780−1790.
(31) Nilwanna, K.; Sittiwong, J.; Boekfa, B.; Treesukol, P.; Boonyaudtayan, S.; Probst, M.; Maihom, T.; Limtrakul, J. Aluminum-based metal-organic framework support metal(II)-hydride as catalyst for the hydrogenation of carbon dioxide to formic acid: A computational study. *Mol. Catal.* **2023**, *541*, 113116.
(32) Sittiwong, J.; Opasmongkolchai, O.; Srifa, P.; Boekfa, B.; Treesukol, P.; Sangthong, W.; Maihom, T.; Limtrakul, J. Computational study of the conversion of methane and carbon dioxide to acetic acid over NU-1000 metal-organic framework-supported single-atom metal catalysts. *Mol. Catal.* **2023**, *535*, 112855.
(33) Schaate, A.; Roy, P.; Godt, A.; Lippke, J.; Waltz, F.; Wiebcke, M.; Behrens, P. Modulated synthesis of Zr-based metal-organic frameworks: From nano to single crystals. *Chem.—Eur. J.* **2011**, *17* (24), 6643−6651.
(34) Valenzano, L.; Civalleri, B.; Chavan, S.; Bordiga, S.; Nilsen, M. H.; Jakobsen, S.; Lillerud, K. P.; Lamberti, C. Disclosing the complex structure of UiO-66 metal organic framework: A synergic combination of experiment and theory. *Chem. Mater.* **2011**, *23* (7), 1700−1718.
(35) Øien, S.; Wragg, D.; Reinsch, H.; Svelle, S.; Bordiga, S.; Lamberti, C.; Lillerud, K. P. Detailed structure analysis of atomic positions and defects in zirconium metal-organic frameworks. *Cryst. Growth Des.* **2014**, *14* (11), 5370−5372.
(36) Zhao, Y.; Truhlar, D. G. The M06 Suite of Density Functionals for Main Group Thermochemistry, Thermochemical Kinetics, Noncovalent Interactions, Excited States, and Transition Elements: Two New Functionals and Systematic Testing of Four M06-Class Functionals and 12 Other Functionals. *Theor. Chem. Acc.* **2008**, *120* (1−3), 215−241.
(37) Zhao, Y.; Truhlar, D. G. Benchmark Data for Interactions in Zeolite Model Complexes and Their Use for Assessment and Validation of Electronic Structure Methods. *J. Phys. Chem. C* **2008**, *112* (17), 6860−6868.
(38) Řezáč, J.; Fanfrlík, J.; Salahub, D.; Hobza, P. Semiempirical quantum chemical PM6 method augmented by dispersion and H-bonding correction terms reliably describes various types of noncovalent complexes. *J. Chem. Theory Comput.* **2009**, *5* (7), 1749−1760.
(39) Frisch, M. J.; Trucks, G. W.; Schlegel, H. B.; Scuseria, G. E.; Robb, M. A.; Cheeseman, J. R.; Scalmani, G.; Barone, V.; Mennucci, B.; Petersson, G. A.; Nakatsuji, H.; Caricato, M.; Li, X.; Hratchian, H. P.; Izmaylov, A. F.; Bloino, J.; Zheng, G.; Sonnenberg, J. L.; Hada, M.; Ehara, M.; Toyota, K.; Fukuda, R.; Hasegawa, J.; Ishida, M.; Nakajima, T.; Honda, Y.; Kitao, O.; Nakai, H.; Vreven, T.; Montgomery, J. A., Jr; Peralta, J. E.; Ogliaro, F.; Bearpark, M.; Heyd, J. J.; Brothers, E.; Kudin, K. N.; Staroverov, V. N.; Kobayashi, R.; Normand, J.; Raghavachari, K.; Rendell, A.; Burant, J. C.; Iyengar, S. S.; Tomasi, J.; Cossi, M.; Rega, N.; Millam, J. M.; Klene, M.; Knox, J. E.; Cross, J. B.; Bakken, V.; Adamo, C.; Jaramillo, J.; Gomperts, R.; Stratmann, R. E.; Yazyev, O.; Austin, A. J.; Cammi, R.; Pomelli, C.; Ochterski, J. W.; Martin, R. L.; Morokuma, K.; Zakrzewski, V. G.; Voth, G. A.; Salvador, P.; Dannenberg, J. J.; Dapprich, S.; Daniels, A. D., Farkas, O.; Foresman, J. B., Fox, D. J. *Gaussian 09*, Rev. D.01.; Gaussian Inc.: Wallingford CT, 2010.
(40) Timofeeva, M. N.; Panchenko, V. N.; Lukoyanov, I. A.; Jhung, S. H. Zirconium-containing metal organic frameworks as solid acid catalysts for the N-formylation of aniline with formic acid. *React. Kinet. Mech. Catal.* **2021**, *133*, 355−369.

https://doi.org/10.1021/acsomega.3c06624
ACS Omega 2023, 8, 46904−46913